Biochimica et Biophysica Acta, 689 (1982) 249–260
Elsevier Biomedical Press

BBA 71273

ON THE FUNCTIONAL SYMMETRY OF NUCLEOSIDE TRANSPORT IN MAMMALIAN CELLS

ROBERT M. WOHLHUETER and PETER G.W. PLAGEMANN

Department of Microbiology, University of Minnesota, Medical School, Minneapolis, MN 55455 (U.S.A.)

(Received October 19th, 1981)

Key words: Nucleoside transport; Transport symmetry; (Mammalian cell)

The transport of uridine and thymidine has been examined in HeLa cells, in Novikoff rat hepatoma cells and in human erythrocytes, with the purpose of comparing influx, efflux and isotopic exchange at chemical equilibrium. The results support the following conclusions: (i) In all three cell types influx and efflux are comparable; (ii) HeLa and Novikoff cells show no *trans*-effect, while erythrocytes show a 5-fold *trans*-stimulation; (iii) a single kinetic entity accounts for nucleoside transport in HeLa and Novikoff cells – no parallel routes of permeation with $K_m < 40$ μM were detected. For the cultured cells, the flux data conform to the kinetic model of a single, carrier-mediated transport system symmetrical with respect to direction, and with equal mobilities of substrate-loaded and empty carrier.

Introduction

In recent years it has become clear that cultured mammalian cells generally possess a transport system for nucleosides characterized by relatively low affinity (half-saturation > 100 μM) and broad substrate specificity. In all cell lines where such a low-affinity system has been characterized, it has proved to be remarkably rapid; the half-times for attainment of transmembrane equilibrium at 25°C are typically on the order of 6 s. The methodological challenges posed by the rapidity of the transport systems have been met in a variety of ways.

The true characteristics of nucleoside transport are most readily appreciated in experimental systems in which transport is not complicated by metabolism of the permeant. Much of the kinetic information on nucleoside transport has been gathered in cells deficient in nucleoside kinases, in cells depleted of ATP, in cells whose adenosine deaminase has been inhibited, or in untreated, wild-type cells with artificial, non-metabolized permeants. (For a review of the literature see Refs. 1 and 2.)

If, by these or other means, a transport system can be isolated kinetically, it becomes feasible to examine flux data in terms of theoretical models of transport. In fact, we have found that thymidine influx into Novikoff hepatoma cells is reasonably well described by an integrated rate equation corresponding to a simple, carrier-mediated model of transport [3] in which carrier mobility is assumed symmetrical with respect to direction and equal for substrate-loaded and free carrier [4]. Accordingly, we have used that equation, along with its implicit assumptions, to evaluate the kinetic parameters of transport for a number of other cell/permeant combinations.

Our purposes in the present study are three-fold. (i) We examine more closely the conformity of nucleoside transport to this simple, theoretical model, by testing directly some of the assumptions of our simple model, viz. directional symmetry of transport, equal mobility of loaded and empty carrier, and the lack of parallel routes of permeation. (ii) We look with greater statistical rigor than heretofore at the goodness of fit of the integrated rate equations. (iii) We include, in addition to

Novikoff cells, HeLa cells and human erythrocytes, both of which cell types have been popular objects of transport studies.

Materials and Methods

Cells. HeLa cells were propagated in spinner culture in Eagle's minimal essential medium for suspension culture supplemented with 10% (v/v) fetal bovine serum inactivated at 56°C. Novikoff rat hepatoma cells were grown in Swim's medium 67 on a gyratory shaker. Cells were enumerated with a Coulter counter, and their viability was assessed by staining with Trypan blue. Our stock cultures were examined periodically for mycoplasma by the uridine/uracil incorporation method [5]. No mycoplasma contamination was detected.

As in previous studies [6], a thymidine kinase-deficient subline (1-4-14, under 1% wild-type activity) of Novikoff cells was employed with thymidine as permeant, and uridine kinase-deficient subline (1-14-6) with uridine as permeant. Nucleoside kinase-negative mutants of HeLa cells were, however, not available to us, so we resorted to the use of cells depleted of ATP and thus unable to phosphorylate imported nucleosides. HeLa cells were depleted of ATP by treatment with 5 mM KCN plus 5 mM iodoacetate for 15 min at 37°C in basal medium devoid of glucose [6,7]. Treated cells were checked for Trypan blue exclusion and normal size distribution at the end of each experiment.

Fresh human erythrocytes were obtained as a byproduct of lymphocyte harvest in the laboratory of Richard Estensen. They were washed four times in isotonic saline and resuspended in Eagle's minimal essential medium for transport measurements.

Transport measurements. Our techniques for measuring transport have been described in detail [4,7,8]. Cell suspensions are mixed with substrate solution (448 μl:61 μl) by means of a dual syringe device; the mixture is delivered to tubes mounted in an Eppendorf microcentrifuge and containing 200 μl of a silicone oil of density intermediate between the aqueous medium and the cells. Uptake is terminated by starting the centrifuge. The effective delay in removing cells from medium is 2 s [7]; thus, the earliest practicable exposure time is 2.2 s, followed by 11 additional samples at, at least, 1 s intervals.

Variations in this procedure permit several experimental protocols. Zero-*trans* influx is arranged by mixing washed cells with radioactive substrate. Equilibrium exchange is arranged by preincubating cells with a given concentration of substrate, then mixing with radiolabeled substrate at the same concentration. Efflux is arranged by preloading cells with radiolabeled substrate and mixing them from the smaller syringe (61 μl) with substrate-free medium (448 μl). This case corresponds to a 'finite-*trans*' protocol, in that, at zero time, the exogenous concentration of substrate is 1/8.3-times the intracellular concentration. The actual protocol used in each experiment is defined in figure legends.

With each protocol, it is the intracellular concentration of radioactivity which is measured as a function of time. This is corrected for extracellular water space in the pelleted cells, and normalized to intracellular water space, as measured by [^{14}C]inulin and $^{3}H_2O$, respectively [7]. Exceptions are noted in figure legends.

Erythrocytes required slight modification of the experimental operations which we had developed for use with cultured cells. To avoid scintillation quenching by hemoglobin an aliquot of the colorless, trichloroacetic acid supernate from pelleted cells, rather than the entire pellet, was used to quantitate intracellular radioactivity.

Evaluation of data. Even at the earliest sampling times we can achieve (see, for example, Fig. 1), a decelerating rate of substrate accumulation is manifest. The pencil-and-ruler approach to evaluating initial velocities of uptake from such data is, therefore, problematic; we have preferred to fit curves to the data. A set of curves which has proved serviceable are the integrated rate equations for zero-*trans* influx and for isotope exchange at chemical equilibrium developed on a simple, symmetrical, carrier-mediated model [3]. Zero-*trans* influx may be expressed:

$$S_{2,t} = S_1\left[1 - \exp\left(-\frac{t/R + (1 + S_1/K)S_{2,t}}{K + 2S_1 + S_1^2/K}\right)\right] \quad (1)$$

where $S_{2,t}$ is the intracellular concentration of

transport substrate at time t, S_1 is the extracellular concentration of substrate and (because of the great excess of extracellular over intracellular volume) is regarded as constant; R is a resistivity term equal to the reciprocal of the maximum velocity of entry, and K is the Michaelis-Menten constant. When $S_1 \ll K$, Eqn. 1 reduces to that for a first-order approach to equilibrium.

An integrated rate equation for the same carrier model, but corresponding to isotope exchange at chemical equilibrium may be expressed in analogous form:

$$N_{2,t} = N_1\left[1 - \exp\left(-\frac{V^{ee}t}{K^{ee}+S}\right)\right] \quad (2)$$

where N is the specific radioactivity of substrate in the compartment designated by the subscripts as for Eqn. 1. For purposes of comparison of exchange and influx data, N may be regarded as the concentration of isotopic substrate at its initial specific radioactivity.

Eqns. 1 and 2 are potentially very informative. Given a set of influx data comprising a wide range of times and permeant concentrations, for example, Eqn. 1 can be fitted by a least-squares procedure to these data to yield directly estimates of the kinetic parameters of influx (viz. K and R). This approach is 'potentially' informative, in the sense that the parameter values thus obtained are quite sensitive to the appropriateness of the model, i.e., to the validity of the assumptions implicit in the model: directional symmetry, equal mobility of loaded and empty carrier, metabolic inertness of the substrate, and the existence of only a single mode of transport. We have used Eqns. 1 and 2 in this capacity in the past, and do so here, for instance, to evaluate the data of Fig. 1.

To examine the validity of the assumptions implicit in Eqns. 1 and 2, we rely on direct comparisons of plotted flux data.

Chromatographic procedures. Uridine and uracil were separated chromatographically on Whatman 3MM paper with a solvent composed of 66 ml *n*-butanol and 34 ml H_2O (solvent 30). Uridine and uracil nucleotides were separated with a solvent composed of 30 ml 1 M ammonium acetate, pH 5, plus 70 ml 95% ethanol (solvent 28; Ref. 9).

Materials. Isotopes were purchased from the following sources: [5-^{3}H]uridine from New England Nuclear (Boston, MA) or Moravek Biochemicals (Brea, CA); [*methyl*-^{3}H]thymidine from Amersham Corp. (Arlington Heights, IL); [*carboxyl*-^{14}C]carboxyinulin and ^3H_2O from New England Nuclear. The specific activity of the nucleosides was diluted by addition of non-labeled compound as indicated in figure legends. Silicone fluid No. 550 was obtained from Dow-Corning Corp. (Midland, MI).

Results and Discussion

The high-K_m nucleoside transport system

The thymidine transport system of Novikoff hepatoma cells has been kinetically characterized in an earlier publication [4]. Analogous studies of uridine transport in HeLa cells are presented in Fig. 1. Panels A–F illustrate the time-courses of uridine accumulation in ATP-depleted HeLa cells at 25°C under zero-*trans* conditions. Chromatographic analysis of the acid-soluble pools of the cells and culture fluid showed that the uridine phosphorylation and phosphorolysis were negligible during the time period of measurements (data not shown). The symmetrical, integrated zero-*trans* influx equation (Eqn. 1) was fitted to the data pooled for eight uridine concentrations (20–2560 μM); the best-fitting values of K and V were 206 ± 13 μM and 54 ± 1.2 pmol/μl cell water per s, respectively.

The corresponding first-order rate constant ($k' = V/K = 0.26$ s^{-1}) implies that, at $S_1 \ll K$, half-equilibrium was attained by 2.7 s. The rapidity of uridine transport in HeLa cells is thus comparable to that observed with uridine and other nucleosides in several cultured cell lines (see Ref. 1 for a tabulation).

We had earlier reported a Michaelis-Menten constant for uridine transport in HeLa cells of 84 μM [10]. That value was based on graphical analysis of uptake data, which we now know to underestimate Michaelis-Menten constants. Many of the data from that publication have been recalculated by our current methods, and the revised values can be found in Plagemann and Wohlhueter [1]. Reevaluation of the data for HeLa cells was not included there; the revised values are $K = 199 \pm 7$ μM and $V = 15 \pm 0.2$ pmol/μl cell water per s.

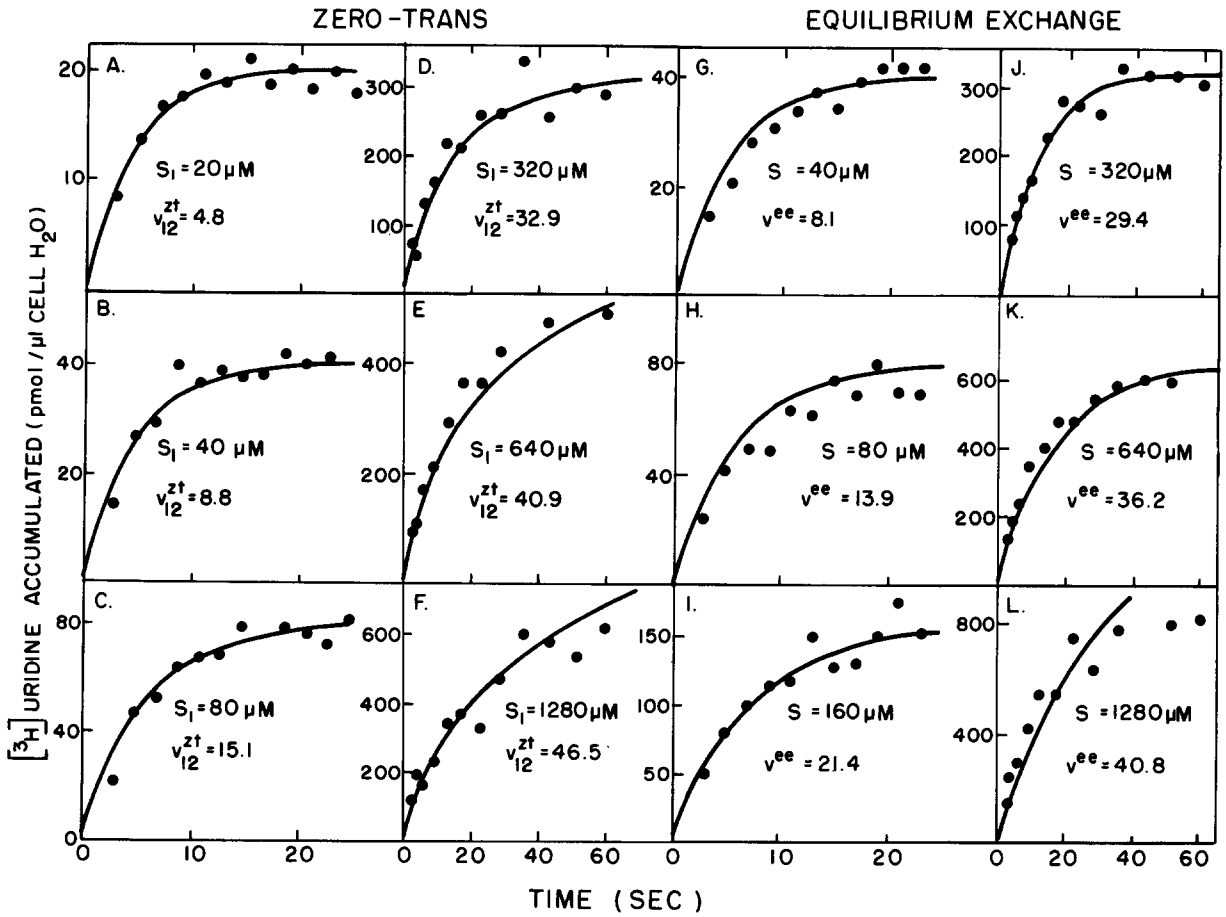

Fig. 1. Zero-*trans* entry (A–F) and inward equilibrium exchange (G–L) of uridine in ATP-depleted HeLa cells at 25°C. Time-courses of radioactivity accumulation to transmembrane equilibrium from 20, 40, 80, 160, 320, 640, 1280 and 2560 μM [^{3}H]uridine (650 cpm/μl, irrespective of concentration) were determined by the rapid kinetic technique as described in Materials and Methods. The zero-*trans* and equilibrium exchange experiments were conducted with the same cell suspension and in the same manner, except that in the equilibrium exchange protocol samples of cell suspension were preloaded with the same concentration of unlabeled uridine at 37°C for 20 min. Radioactivity/cell pellet was corrected for uridine trapped in extracellular space (1.5 μl/pellet) and converted to pmol/μl cell water on the basis of an intracellular water space of 5.6 μl/pellet. In the case of the equilibrium exchange the oridinate pertains to radiolabeled uridine. Eqn. 1 was fitted by the method of least squares to the pooled zero-*trans* influx data. The best fitting parameters were $K = 206 \pm 13$ μM and $V = 54 \pm 1.2$ pmol/μl cell water per s ($r_{y,\hat{y}} = 0.987$). The theoretical curves for $S_1 = 20$, 40, 80, 320, 640 and 1280 μM are illustrated in frames A–F. The initial transport velocities (v_{12}^{zt}) were calculated $v_{12}^{zt} = \frac{S_1/R}{K + S_1}$. Eqn. 2 was fitted by the method of least squares to the pooled equilibrium exchange data. The best fitting parameters were $K^{ee} = 191 \pm 38$ μM and $V^{ee} = 47 \pm 2.6$ pmol/μl cell water per s ($r_{y,\hat{y}} = 0.979$). The theoretical curves for $S = 40$, 80, 160, 320, 640 and 1280 μM are illustrated in frames G–L. Initial velocities (v^{ee}) were calculated as $v^{ee} = \frac{V^{ee}S}{K^{ee} + S}$.

Thus, the Michaelis-Menten constant observed by us 3 years ago was the same as that observed here, while the velocity was much less. We have experienced considerable variation in maximal velocities of transport from batch-to-batch of other cell types as well, and do not know the cause of the variability.

Zero-*trans* influx of thymidine was measured in HeLa cells in an experiment analogous to that of Fig. 1. Best fitting kinetic parameters were $K = 183 \pm 24$ μM and $V = 44 \pm 2.2$ pmol/μl cell water per s ($k' = 0.24$ s^{-1}). This value of K is similar to that for thymidine transport observed in Novikoff cells (228 μM; Ref. 4) and in a number of cell lines

TABLE I

INHIBITION OF THYMIDINE AND URIDINE INFLUX BY EACH OTHER AND ADENOSINE IN ATP-DEPLETED HeLa CELLS AT 25°C

[a] The time courses of radioactivity accumulation from 320 μM [^{3}H]thymidine (316 cpm/μl) or 320 μM [^{3}H]uridine (320 cpm/μl) were determined by the rapid kinetic technique as described in Materials and Methods. Initial velocities of transport were computed by fitting Eqn. 1 with K fixed at 200 μM and taking the slope at zero time. Where indicated, unlabeled thymidine, uridine or adenosine were added simultaneously with labeled substrate to a final concentration of 2 mM. Radioactivity per cell pellet was corrected for substrate trapped in inulin-accessible, extracellular space (4.4 and 4.0 μl/pellet in the thymidine and uridine experiments, respectively) and converted to pmol/μl cell H_2O on the basis of intracellular H_2O spaces of 13.9 and 11.9 μl/pellet, respectively.

Unlabeled nucleosides (2 mM)	Thymidine		Uridine	
	V_{12}^{zt} (μM/s)	Inhibition (%)	V_{12}^{zt} (μM/s)	Inhibition (%)
None	52.7±0.62	0	25.9±4.5	0
Thymidine	6.9±0.60	87	3.3±0.4	87
Uridine	7.0±0.62	85	5.0±0.5	81
Adenosine	4.8±0.34	91	1.9±0.3	92

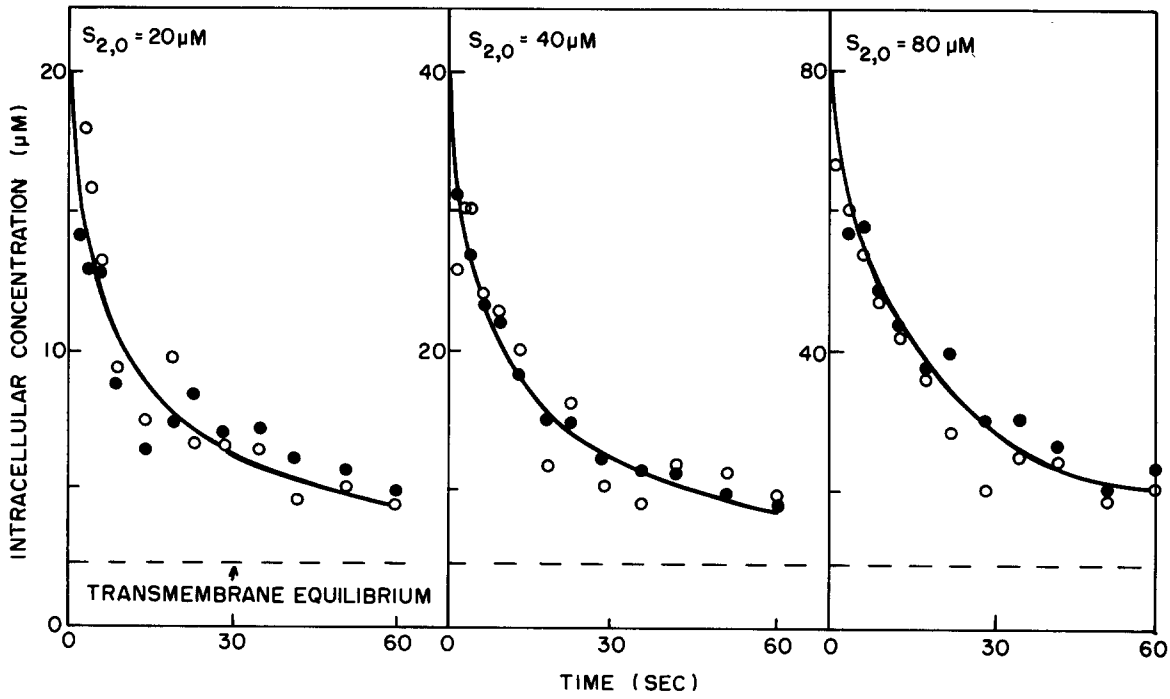

Fig. 2. Lack of *trans*-acceleration of thymidine efflux from Novikoff cells. A suspension of cells of subline 1-4-14 (thymidine kinase deficient) were incubated with [*methyl*-^{3}H]thymidine (2660 cpm/μl) at the concentrations indicated for about 10 min at 37°C, and then brought to 25°C for efflux measurements. The cell suspension was mixed by means of a dual syringe device either with basal medium devoid of thymidine (○, 'zero-*trans*') or with non-radioactive thymidine at 10 mM (S_1) (●, 'infinite-*trans*'). The cell pellets contained 1.3 μl extracellular water and 6.0 μl intracellular water. The curves are hand drawn.

including an earlier report for HeLa cells ($K = 125 \pm 5$ μM; see Ref. 4), while, as with uridine, V was substantially higher (cf. $V = 8.2 \pm 0.1$ pmol/μl cell water per s) for the current batch of cells.

Specificity of the high-K_m system of HeLa cells

The kinetic similarities between transport of uridine and thymidine in HeLa cells suggest the possibility that a single system may transport both substrates. This conclusion is substantiated by the results presented in Table I. Addition of unlabeled thymidine, uridine or adenosine simultaneously with radioactive substrate inhibited influx of the latter. The magnitude of inhibition was the same whether [^{3}H]thymidine or [^{3}H]uridine served as substrate. Adenosine was a somewhat stronger inhibitor than either pyrimidine nucleoside, consistent with the generally higher affinities of purine nucleosides for the nucleoside transporters of other cell lines [1,8]. Thus, it seems most likely that the high-K_m, thymidine/uridine transport system of HeLa cells, as in Novikoff rat hepatoma cells [4], RPMI 6410 cells [11], P388 leukemia cells [8] and erythrocytes [12] is a broadly specific nucleoside carrier.

Lack of trans effect on the high-K_m system of cultured cells

In contrast to the zero-*trans* protocol, the equilibrium exchange protocol involves discrete concentrations of (non-isotopic) permeant at the *trans* face of the membrane. Comparisons of zero-*trans* and equilibrium exchange fluxes thus reveal any *trans* effect of permeant on the flux from the *cis* side. Representative time-courses of inward equilibrium exchange of uridine into HeLa cells are illustrated in panels G–L of Fig. 1. It is apparent from the graphs that the initial velocities of entry and exchange at the same substrate concentration were comparable, i.e., there was no obvious *trans*-effect of unlabeled substrate present at the inner face of the membrane. This lack of *trans*-effect confirms one of the assumptions implicit in Eqns. 1 and 2.

Fitting Eqn. 2 to the exchange data pooled for all eight substrate concentrations yielded estimates of $K^{ec} = 191 \pm 38$ μM and $V^{ec} = 47 \pm 2.6$ pmol/μl cell water per s, values which are indistinguishable from the estimates of K and V obtained in the zero-*trans* experiments. Similar results were obtained previously for thymidine influx in Novikoff cells [4]. Such results are interpreted in terms of the simple carrier model as evidence for equal mobilities of the carrier, whether loaded with substrate or empty.

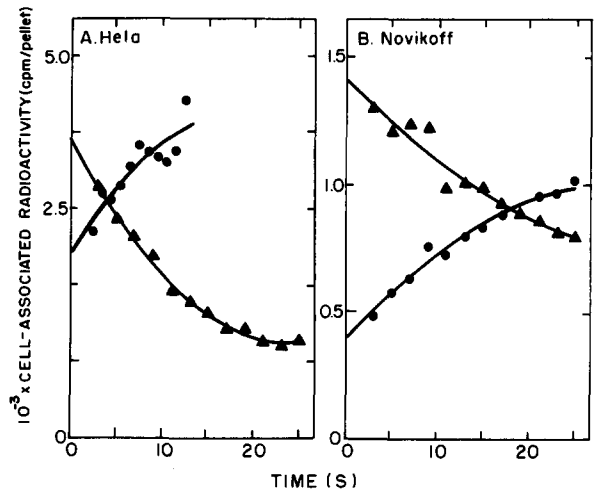

Fig. 3. Equality of thymidine influx and efflux in ATP-depleted HeLa cells (panel A) and thymidine kinase-deficient Novikoff hepatoma cells (panel B). To measure efflux, cells were preloaded with 200 μM thymidine (approx. 1.6 cpm/pmol), diluted 8.31-times into nucleoside-free medium by means of a dual syringe mixer (initial exogenous concentration, 24 μM), and centrifuged through oil after incubation (24°C) for the times indicated on the abscissa. To measure influx, cells were preloaded with 24 μM nucleoside, diluted 1.14-times into medium containing 1662 μM nucleoside (initial exogenous concentration, 200 μM), and centrifuged through oil. The ordinate represents radioactivity recovered in the cell pellet expressed as cpm per cell pellet (10.4 and 4.0 μl per pellet for panels A and B, respectively). Initial slopes of the curves shown were estimated graphically to be about 190 and -230 cpm/s per pellet for influx and efflux in HeLa cells, and 39 and -36 cpm/s per pellet for influx and efflux in Novikoff cells.

Lack of *trans*-effect pertained also to efflux of permeant. This is demonstrated in Fig. 2 for thymidine efflux from thymidine kinase-deficient Novikoff cells. The presence of 10 mM thymidine ('infinite-*trans*' protocol) had no influence on the efflux of isotopic thymidine.

Directional symmetry of transport in cultured cells

A second assumption implicit in Eqn. 1 is that of directional symmetry of the transporter. This assumption, too, has been tested by direct observa-

tion of influx versus efflux of nucleosides. The results are reported in Fig. 3, in which are plotted influx and efflux data for thymidine in ATP-depleted HeLa cells and for thymidine-kinase-deficient Novikoff cells.

In the efflux mode our dual syringe technology results necessarily in a finite concentration ratio (8.3) across the cell membrane at time zero. In order to compare directly isotope influx with efflux, we designed these experiments to establish this same concentration ratio across the membrane, but in opposite senses, for both influx and efflux measurements. The greater of the two concentrations (200 μM) was chosen close to the K_m for transport, so that asymmetries with respect to either maximum velocity or substrate affinity would be registered.

For the experiments portrayed in Fig. 3, efflux and influx for both cell types were obviously comparable. In a total of five such experiments, however, our graphical analysis indicated that efflux exceeded influx by about 1.5-fold on the average. Whether this slight asymmetry is real, or a consequence of systematic errors of measurement, is not clear. In any case, it is of little consequence: theoretically, it is of minor interest compared to the 10-fold difference in mobility of the loaded and unloaded erythrocyte carrier (see below); practically, it does not seriously compromise the use of Eqns. 1 and 2 in evaluating kinetic data obtained from these cells. For example, imposition of a 1.5-fold, in/out asymmetry in the evaluation of the data of Fig. 1 leads to a K value of 209 μM, compared to 206 μM obtained by use of the symmetrical equation.

Similar experiments were undertaken also with uridine as permeant, and indicated roughly equal influx and efflux in ATP-depleted HeLa cells and uridine-kinase-deficient Novikoff cells. The interpretation of these results, however, was complicated by the extensive phosphorolysis of uridine which occurred during the preloading period. Chromatographic analysis of acid extracts of the Novikoff cells showed that, after 10 min preloading with 200 μM [^{3}H]uridine, 48% of the cell-associated radioactivity was uracil (none was UXP).

Symmetry relationships in erythrocytes

The observations reported here, together with

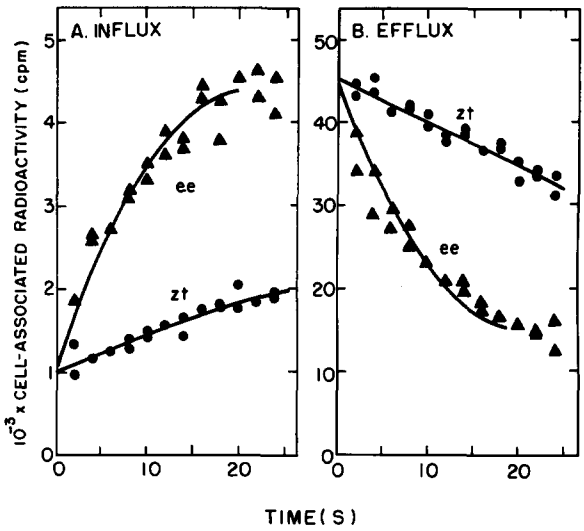

Fig. 4. Symmetry relationships of the uridine carrier of erythrocytes. Four modes of transport were examined in human erythrocytes at a presumably saturating concentration of uridine (4 mM): inward equilibrium exchange (panel A, 'ee',▲), outward equilibrium exchange (panel B, 'ee', ▲), zero-*trans* influx (panel A, 'zt', (●) and efflux (designated 'zt', (●) in panel B, but actually efflux into medium containing 0.48 mM uridine at zero time). Specific radioactivities were 84.1 and 573 cpm/nmol for panels A and B, respectively. Dual syringe mixing was employed as described in Methods; ambient temperature was 25°C. Cell pellets were extracted with 800 μl 0.5 M trichloroacetic acid, the mixture centrifuged, and a 400 μl aliquot of the clear supernate counted. The aliquots were equivalent to 15 μl intracellular water and 2.5 μl extracellular water. The slopes of the curves at time zero were estimated graphically and corrected for specific radioactivity. They correspond to velocities (pmol/μl cell water per s) of about 40 and 200 for zt and ee influx, respectively, and 40 and 330 for zt and ee efflux, respectively.

our previous studies (summarized in Ref. 1) represent the only attempts we know of to assess the directional symmetries and differential carrier mobilities of nucleoside transport systems in cultured cells. Our conclusions with respect to cultured cells, however, do not accord with results reported for erythrocytes, which indicate a marked *trans*-stimulation [13–15] and directional asymmetry [15].

It seemed appropriate, therefore, to test our methodology also on the erythrocyte system. Influx, efflux and exchange of a presumably saturating concentration (4 mM) of uridine were measured in erythrocytes maintained at 25°C. The

results are depicted in Fig. 4. Zero-*trans* influx and efflux (V_{12}^{zt} and V_{21}^{zt}) at this concentration were comparable, indicative of directional symmetry. In their exhaustive kinetic analysis of uridine transport in human erythrocytes, Cabantchik and Ginsburg [15] reported directional asymmetry, with V_{12}^{zt}/V_{21}^{zt} in the range of 0.3–0.5. Our studies of nucleoside transport in erythrocytes are incomplete, and we hesitate, on the basis of the present data, to argue the incorrectness of Cabantchik and Ginsburg's conclusion. We are pursuing these studies further in an effort to resolve the discrepancy.

The relative velocities of equilibrium exchange and zero-*trans* flux depicted in Fig. 4 are consistent with the more complete analysis by Cabantchik and Ginsburg [15] and by Paterson and colleagues [13,14]. Whether measured in the inward or outward direction, exchange flux was at least 5-times as rapid as zero-*trans* flux. The magnitude of this *trans*-effect, interpreted in terms of a simple carrier, implies a differential mobility of loaded and empty carrier of about 10-fold.

The differential mobilities of loaded and empty carrier seen in erythrocytes contrast with the equal mobilities observed in the cultured cell lines. The contrast serves as a sort of positive control on our methodology, and it demonstrates that differential mobilities are not an inherent property of mobile carrier transport systems.

On the absence of a low-K_m system in HeLa cells

The results with cultured cells thus far confirm the symmetry assumptions implicit in Eqns. 1 and 2, but have not addressed an even more fundamental assumption: that we are dealing with a single transport system. Our choice of substrate concentration range, as exemplified in Fig. 1, and our curve-fitting program's inability to accomodate multiple sets of kinetic parameters, may have caused us to overlook the existence of a second transport system of substantially lower K_m. Our attempts to exclude this possibility have focussed on HeLa cells, since nucleoside uptake in this cell type has often been interpreted to indicate low-K_m transport systems, with Michaelis-Menten constants of about 0.5 μM for thymidine, 3.6 μM for adenosine and 6 μM for uridine [2,16–23].

We have examined this problem in two ways.

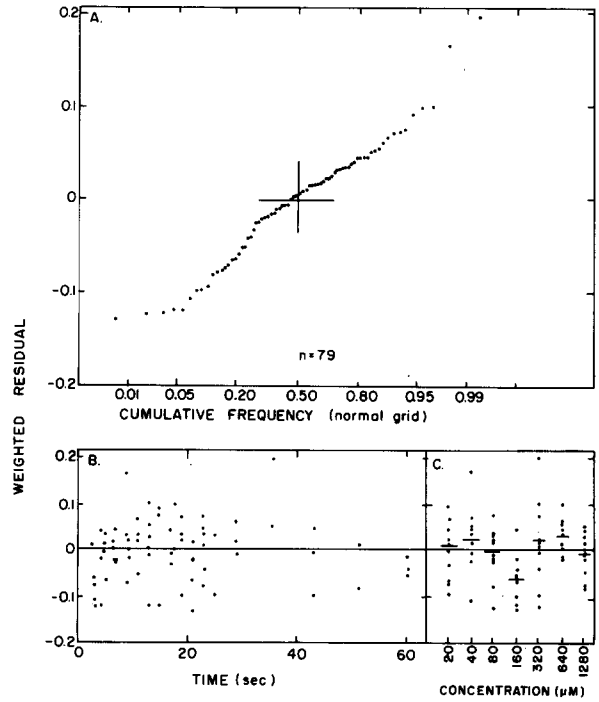

Fig. 5. Examination of residuals generated by fitting a single-component equation to uridine transport data. The best fitting rate curves obtained by fitting Eqn. 1 to the uridine uptake data are shown in Fig. 1. The weighted residuals from that fit [($y_{observed} - y_{theoretical}$)/exogenous concentration] are displayed in three formats. Panel A is the cumulative frequency plotted on a normal grid. Normal distributions thus plotted conform to a straight line passing through the point marked by the cross. Panel B shows the same residuals plotted against one of the independent variables (time). Panel C shows the residuals grouped by exogenous substrate concentration, the second independent variable. The horizontal lines indicate the means of each group.

First, and most directly, we have measured initial rates of uridine entry into ATP-depleted HeLa cells at six concentrations in the 0.1–40 μM range, the range in which a low-K_m system is expected. The usual 12 samples were taken over a span of 18.5 s, and initial velocities were calculated in a non-prejudicial way from the individual uptake curves, namely as the initial slope of an exponential curve fit to the data. (As can be appreciated from Fig. 1, such sampling times do not comprise a linear segment of the uptake curve. In fact, linear regressions on the initial samples to 8 s were roughly proportional to the initial slopes of the exponential curve but underestimated these by

65% on the average.) The zero-time slopes thus calculated were plotted against substrate concentration (plot not shown). Within this range of concentration velocity was strictly first-order with respect to uridine; the first-order rate constant was $k' = 0.28\ s^{-1}$ (compare $k' = 0.26\ s^{-1}$ calculated from the kinetic parameters determined in Fig. 1). Thus, uridine uptake in this low range of concentration appears to be fully accounted for by operation of the high-K_m transport system.

Analogous studies were performed also with thymidine kinase-deficient and ATP-depleted Novikoff cells and with uridine in uridine kinase-deficient and ATP-depleted Novikoff cells. No saturation was evident in any of these systems. We had examined adenosine transport in P388 leukemia cells in a similar manner and came to the same conclusion [8].

Our second approach to the question of additional transport components is a statistical one. If our application of Eqn. 1 to the evaluation of kinetic constants is biased against detection of a coexisting, low-K_m mechanism, then the examination of the residuals ($Y_{observed} - Y_{theoretical}$) should reveal that bias as a departure from a normal distribution of residuals or as a tendential change of them with the independent variables t and S_1. The residuals associated with the zero-*trans* fit of Fig. 1 are reproduced as Fig. 5. The residuals conform reasonably well to a normal distribution (panel A; see Ref. 24 for examples of normal populations plotted in this format). There was no obvious correlation of residuals with the time variable (panel B). Residuals grouped by substrate concentration (panel C) are not centered on zero for each group, but the group averages are random about zero. The failure of each group to center at zero would result, for example, from inaccuracies in substrate concentrations relative to one another.

Taken together, we believe these investigations leave little room for any significant contribution to uridine transport in ATP-depleted HeLa cells by systems other than the high-K_m transporter characterized above or to thymidine and uridine transport in Novikoff cells. This conclusion leaves open the possibility that treatment with KCN and iodoacetate obliterates a second transport system of HeLa cells. This is a question which is difficult for us to address, because we have no nucleoside kinase-negative mutants of this line. We have, however, ruled out this possibility in Novikoff hepatoma cells, where no saturation was seen in KCN-iodoacetate-treated cells or in kinaseless cells. We had reported previously that, overall, the kinetics of thymidine transport in a thymidine kinase-negative mutant were similar (and comparable to that described here for HeLa cells) whether or not the cells were treated with KCN and iodoacetate [4]. Furthermore, it is shown below that even in untreated HeLa cells, the initial rates of entry, albeit poorly defined ones, did not saturate in the low concentration range.

Transport studies in metabolically active cells

We subscribe to the premise that a truly initial, linear rate of uptake of a nucleoside in cells metabolizing that nucleoside is a valid measure of transport. However, the reality of nucleoside transport, as evidenced in this report and many others (see Ref. 1), lays very considerable technical stumbling blocks to the measurement of truly initial rates and to the rigorous demonstration that apparently initial rates are not influenced by metabolic processes. We have discussed these problems from a theoretical viewpoint elsewhere [25].

In metabolically active cells the contribution to uptake of transport and phosphorylation can be dissected kinetically [10,26–28]. To this end, HeLa cells exposed to labeled substrate were centrifuged through silicone oil into an underlying aqueous layer containing 10% trichloroacetic acid. The chemical form of the cell-associated radioactivity was then determined by chromatographic means. Fig. 6 illustrates the results of such an experiment at 1 and 100 μM uridine. At the lower concentration, intracellular free uridine reached a steady state by about 10 s (Fig. 6A). Thereafter, the rate of accumulation of intracellular radioactivity reflected the rate of phosphorylation of uridine, yielding nucleotides which do not permeate the membrane and which are, therefore, trapped within the cell. This rate of nucleotide accumulation was nearly equal to the initial rate, attributable to influx, and it persisted for a couple of minutes. The steady-state concentration attained by uridine appeared higher than predicted from cell water measurements. Whether this results from measuring inaccuracies, from phosphorolytic production

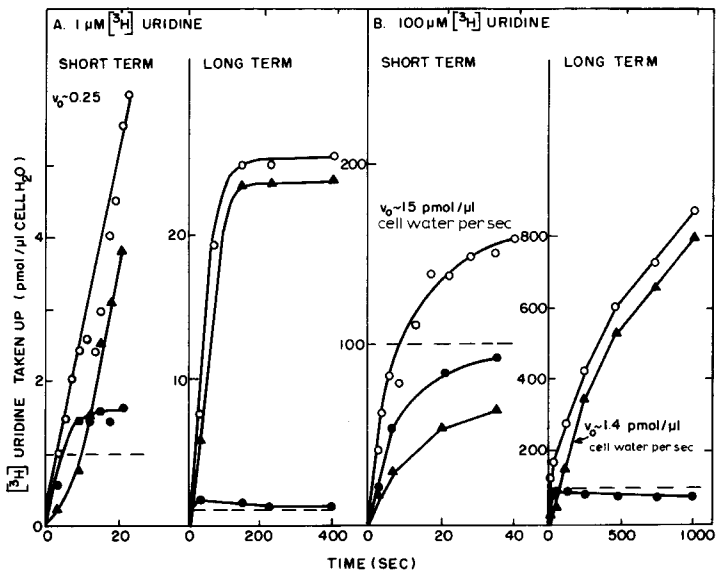

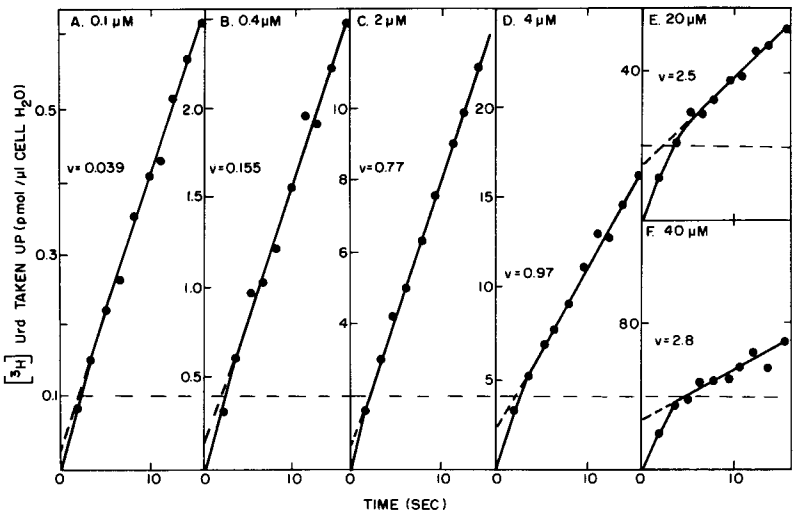

Fig. 6. Uptake of 1 μM (A) and 100 μM (B) of [^{3}H]uridine by untreated HeLa cells at 25°C. The time courses of radioactivity accumulation from 1 or 100 μM [^{3}H]uridine (487 cpm/μl, irrespective of concentration) were determined by the rapid kinetic technique as described in Materials and Methods. Radioactivity/cell pellet was corrected for substrate trapped in extracellular space (6.5 μl/cell pellet) and converted to pmol/μl cell water on the basis of an experimentally determined intracellular H_2O space of 18.6 μl/cell pellet (total, O—O). The cells from duplicate samples were collected by centrifugation through oil into 10% trichloroacetic acid in 10% (w/v) sucrose. Acid extracts were processed and chromatographed with solvent 28 as described in Materials and Methods. The intracellular concentrations of uridine (●—●) and uracil nucleotides (▲—▲) were calculated on the basis of the chromatographic separations and the total amounts of uridine taken up, and were corrected for extracellular uridine trapped in acid extracts. The indicated initial velocities (v_0; in pmol/μl cell water per s) were estimated graphically from the initial linear portions of the appropriate curves.

Fig. 7. Uptake of [^{3}H]uridine in untreated HeLa cells. A suspension of HeLa cells (25°C) was mixed with the indicated concentrations of [^{3}H]Uridine (515 cpm/μl, irrespective of concentration) and centrifuged through silicone as described in Materials and Methods. The centrifuge was started immediately after dispensing the last sample; the acceleration lag was taken as 2 s [4]. Total cell-associated radioactivity was corrected for 2.6 μl extracellular water per pellet and expressed as pmol uridine equivalents per μl of intracellular water (9.9 μl/pellet). The broken line in each panel represents the intracellular concentration of radioactivity equal to that in the medium at zero-time. The uptake velocities noted in each panel (v) were graphically determined for the long-lived kinetic phase (after 3.5 s). An approximate initial velocity was also estimated as the slope from the origin through the first point. Both velocities are replotted as a function of concentration in Fig. 8.

of uracil (which chromatographed with uridine in solvent 28), or from a significantly rapid input into the uridine pool from uracil nucleotide turnover, is not clear.

At 100 μM uridine, the situation was qualitatively similar, but quantitatively distinct in an important way (Fig. 6B). Uridine kinase became saturated after a few seconds, so that the rate of phosphorylation was relatively less predominant until the steady state of free uridine was established at about 40 s. The rate of accumulation of uracil nucleotides in this steady state was only 1/10 that of initial uridine entry.

Fig. 7 extends these studies in phosphorylating cells to a series of uridine concentrations in the range 0.1 to 40 μM. In each case the kinetics of total uptake of isotope were biphasic. The earlier phase was short-lived and poorly defined, but in light of Figs. 1 and 6, it can be ascribed to transport. The later phase, from about 3.5 s onwards, can be ascribed to intracellular phosphorylation of uridine.

One can calculate two velocities from these curves. (i) The well-defined slope of the second kinetic phase, viz. the rate of uridine phosphorylation in situ, and (ii) a rough approximation of the initial velocity of entry, taken as the line from the origin through the first point (approx. 2.2 s). Plots of these velocities against exogenous uridine concentration (Fig. 8) are distinctly different. The curve corresponding to the slope of the second phase conforms well to a Michaelis-Menten curve with $K_m = 8.6$ μM and $V_{max} = 3.5$ pmol/μl cell water per s. We take these values to be the kinetic constants for uridine kinase as it operates in situ. (Compare K_m values reported for uridine uptake of 6 μM [18] to 16 μM [29]).

The curve corresponding to the initial velocities, on the other hand, shows no evidence of saturation, and is somewhat loosely described by a straight line of slope corresponding to a first-order rate constant of 0.35 s^{-1}. (Compare first-order rate constants for uridine transport, Fig. 1 and p. 257, of 0.26–0.28 s^{-1}.)

Intermediate constructions are, of course, possible: the change in cell-associated radioactivity between 2.2 and 9.5 s, if it were construed as 'initial velocity' of transport, would give rise to an apparent K_m of 13 μM.

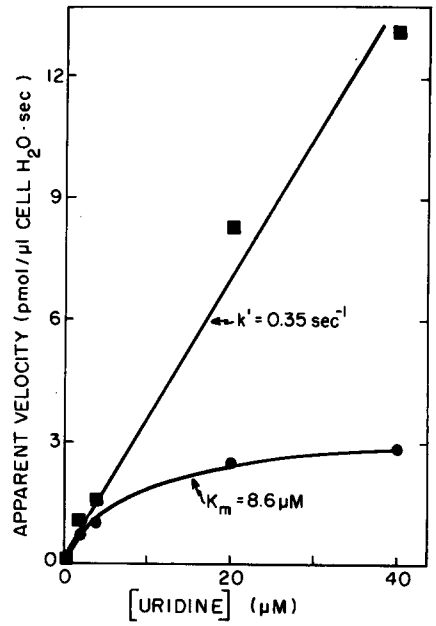

Fig. 8. Velocity versus concentration curves for uridine uptake in untreated HeLa cells. The two sorts of uptake velocities, calculated as described in the legend to Fig. 7, are plotted against exogenous concentration of uridine. Points symbolized by filled circles correspond to the long-term velocity; a Michaelis-Menten curve with $K_m = 8.6 \pm 1.3$ μM and $V_{max} = 3.5 \pm 0.2$ pmol/μl cell water per s is fitted to these points. Points symbolized by squares are the estimated initial velocities; a straight line is fitted to them, corresponding to a first-order rate constant $k' = 0.35 \pm 0.02$ s^{-1}.

From the Michaelis-Menten analysis of the second phase of uptake (Fig. 8) we also conclude that a first-order rate constant of 0.41 s^{-1} (V_{max}/K_m) pertained to the in situ operation of uridine kinase in these cells. As a consequence, the rate of uridine uptake at concentrations in the first-order range of both transporter and uridine kinase (say, less than 4 μM) is in fact determined largely by transport. This fact explains why the biphasic nature of uptake kinetics, so apparent at high concentrations, virtually disappears at low concentrations (Fig. 6). At the higher concentrations uridine kinase no longer operates in the first-order region, it begins to saturate, and phosphorylation becomes rate limiting for uptake.

Acknowledgements

The authors thank John Erbe, Patricia Wilkie, Jill Myers and Carol Lahti for competent technical

assistance, Alan Paterson for supplying a review article [2] prior to publication, and Colleen O'Neill for typing the manuscript. This work was supported by USPHS Research Grant GM 24468.

References

1 Plagemann, P.G.W. and Wohlhueter, R.M. (1980) Curr. Top. Membrane Transp. 14, 226–330
2 Paterson, A.R.P., Kolassa, N. and Cass, C.E. (1981) Pharmacol. Ther. 12, 515–536
3 Eilam, Y. and Stein, W.D. (1974) Methods Membrane Biol. 2, 283–354
4 Wohlhueter, R.M., Marz, R. and Plagemann, P.G.W. (1979) Biochim. Biophys. Acta 553, 262–283
5 Schneider, E.L., Stanbridge, E.J. and Epstein, C.J. (1974) Exp. Cell Res. 84, 311–318
6 Plagemann, P.G.W., Marz, R. and Erbe, J. (1976) J. Cell Physiol. 89, 1–18
7 Wohlhueter, R.M., Marz, R., Graff, J.C. and Plagemann, P.G.W. (1978) Methods Cell Biol. 20, 211–236
8 Lum, C.T., Marz, R., Plagemann, P.G.W. and Wohlhueter, R.M. (1979) J. Cell Physiol. 101, 173–200
9 Plagemann, P.G.W. (1971) J. Cell Physiol. 77, 213–240
10 Plagemann, P.G.W., Marz, R. and Wohlhueter, R.M. (1978) J. Cell Physiol. 97, 49–72
11 Paterson, A.R.P., Yang, W., Lau, E.Y. and Cass, C.E. (1979) Mol. Pharmacol. 16, 900–908
12 Cass, C.E. and Paterson, A.R.P. (1973) Biochim. Biophys. Acta 291, 734–746
13 Oliver, J.M. and Paterson, A.R.P. (1971) Can. J. Biochem. 49, 262–270
14 Pickard, M.A. and Paterson, A.R.P. (1972) Can. J. Biochem. 50, 704–705
15 Cabantchik, Z.I. and Ginsburg, H. (1977) J. Gen. Physiol. 69, 75–96
16 Paterson, A.R.P., Kim, S.C., Bernard, O. and Cass, C.E. (1975) Ann. N.Y. Acad. Sci. 255, 402–411
17 Paterson, A.R.P., Babb, L.R., Paran, J.H. and Cass, C.E. (1977) Mol. Pharmacol. 13, 1147–1158
18 Paterson, A.R.P., Naik, S.R. and Cass, C.E. (1977) Mol. Pharmacol. 13, 1014–1023
19 Cass, C.E. and Paterson, A.R.P. (1977) Exp. Cell. Res. 105, 427–435
20 Lynch, T.P., Cass, C.E. and Paterson, A.R.P. (1977) J. Supramol. Struct. 6, 363–374
21 Lynch, T.P., Lauzon, G.J., Naik, S.R., Cass, C.E. and Paterson, A.R.P. (1978) Biochem. Pharmacol. 27, 1303–1304
22 Cass, C.E., Dahlig, E., Lau, E.Y., Lynch, T.P. and Paterson, A.R.P. (1979) Cancer Res. 39, 1245–1252
23 Paterson, A.R.P., Lau, E.Y., Dahlig, E. and Cass, C.E. (1980) Mol. Pharmacol. 18, 40–44
24 Daniel, C. and Wood, F.S. (1971) Fitting Equations to Data, pp. 33–49, Wiley Interscience, New York
25 Wohlhueter, R.M. and Plagemann, P.G.W. (1980) Int. Rev. Cytol. 64, 171–240
26 Rozengurt, E., Mierzejewski, K. and Wigglesworth, N. (1978) J. Cell. Physiol. 97, 241–252
27 Heichal, O., Ish-Shalom, D., Koren, R. and Stein, W.D. (1979) Biochim. Biophys. Acta 551, 169–186
28 Koren, R., Shohami, E. and Yeroushalmi, S. (1979) Eur. J. Biochem. 95, 333–339
29 Plagemann, P.G.W. and Richey, D.P. (1974) Biochim. Biophys. Acta 344, 263–305